Oxygen Isotope Effect in Superconducting $Ba_{1-x}K_xBiO_3$ from Phonon Density of States

C.-K. Loong

Intense Pulsed Neutron Source, Argonne National Laboratory, Argonne, Illinois 60439

D. G. Hinks,[1] P. Vashishta,[1,3] W. Jin,[1,2] R. K. Kalia,[1,3] M. H. Degani,[1,a] D. L. Price,[1] J. D. Jorgensen,[1] B. Dabrowski,[1,2] A. W. Mitchell,[1,2] D. R. Richards,[1,2] and Y. Zheng[1,2]

[1]*Materials Science Division, Argonne National Laboratory, Argonne, Illinois 60439*

[2]*Science and Technology Center for Superconductivity, Argonne National Laboratory, Argonne, Illinois 60439*

[3]*Concurrent Computing Laboratory for Materials Simulations and Department of Physics, Louisiana State University, Baton Rouge, Louisiana 70803-4001*

(Received 21 December 1990)

The variation of the phonon spectrum of $Ba_{0.6}K_{0.4}BiO_3$ upon oxygen isotope substitution is determined by inelastic neutron scattering (INS). By combining the INS results with molecular-dynamics computer simulation, a value of 0.42 ± 0.05 is obtained for the reference isotope-effect exponent. This is close to the isotope-effect exponent determined from the variation of T_c upon oxygen substitution, indicating that $Ba_{0.6}K_{0.4}BiO_3$ is a weak-coupling superconductor with large matrix elements coupling the electrons to high-energy phonons involving oxygen vibrations.

PACS numbers: 74.20.Fg, 63.20.Kr, 74.70.−b

Since the discovery of superconductivity[1,2] in $Ba_{1-x}K_xBiO_3$, experimental evidence has been accumulating that this compound is simpler than the high-T_c cupric oxides. Showing none of the planar structures observed in other high-T_c compounds, the superconducting phase of $Ba_{1-x}K_xBiO_3$ ($0.37 < x < 0.5$, $T_c \cong 30$ K) in fact displays a cubic perovskite structure.[3] As the dopant concentration is reduced, superconductivity disappears when the structure changes from cubic to orthorhombic. Furthermore, $BaBiO_3$ is nonmagnetic,[4,5] while the other high-T_c related materials, in the parent nonsuperconducting phases, display antiferromagnetism.[6] Hall-effect measurements in $Ba_{1-x}K_xBiO_3$ indicate that the carriers are electrons,[7] whereas in cuprates, with the exception of $R_{2-x}Ce_xCuO_4$ (R = Nd,Pr), the carriers are holes.[8]

The importance of electron-phonon coupling in $Ba_{1-x}K_xBiO_3$ was revealed by measurements of the oxygen isotope-effect exponent for the superconducting transition temperature T_c,

$$\alpha_O = -\frac{\partial \ln T_c}{\partial \ln M_O}, \tag{1}$$

where M_O is the mass of the oxygen isotope. The exponent α_O was found to be 0.41 ± 0.03.[9] Infrared-reflectivity measurements[10] of the superconducting gap Δ in $Ba_{1-x}K_xBiO_3$ give the dimensionless ratio $2\Delta/kT_c = 3.5 \pm 0.4$, consistent with the BCS value of 3.52 for weak-coupling superconductors. Zasadzinski *et al.*[11] have made electron-tunneling measurements on a $Ba_{1-x}K_xBiO_3$/In junction. They find features extending to 60 meV in the tunneling second derivative d^2I/dV^2 corresponding to peaks in the phonon density of states (DOS) obtained by neutron-scattering experiments and molecular-dynamics simulations,[12] implying a strong interaction between electrons and high-energy phonons. Recently, using point-contact junctions, Huang *et al.*[13] have been able to invert the tunneling data to obtain the Eliashberg function $\alpha^2(\omega)F(\omega)$ for $Ba_{1-x}K_xBiO_3$. Their data also show strong features at the same energies as the neutron-scattering measurements.

From the theory of superconductivity,[14–17] the transition temperature of a superconductor can be written as

$$T_c = \langle\omega\rangle \exp[-f(\lambda, \ldots, \mu^*)], \tag{2}$$

where f is a universal functional form determined from the Eliashberg equations. Here we define the characteristic phonon frequency $\langle\omega\rangle$ as the first frequency moment

$$\langle\omega\rangle = \int_0^\infty d\omega\, \omega F(\omega), \tag{3}$$

where $F(\omega)$ is the phonon DOS, λ the electron-phonon coupling constant, and μ^* the Coulomb pseudopotential.

The oxygen isotope-effect exponent defined in Eq. (1) can be written as a sum of two terms obtained by differentiation of Eq. (2):

$$\alpha_O = \alpha_{rO} + \frac{\partial f}{\partial \ln M_O}, \tag{4}$$

where α_{rO} is the "reference" isotope-effect exponent defined by

$$\alpha_{rO} = -\frac{\partial \ln\langle\omega\rangle}{\partial \ln M_O}. \tag{5}$$

For monatomic weak-coupling superconductors, $\alpha_r = \alpha = \frac{1}{2}$. With the presence of strong-coupling effects ($\lambda > 1$), α_r will deviate[18] from α, as observed in Pb and Zn. In multicomponent systems such as $Ba_{1-x}K_xBiO_3$, α_r may be quite different from $\frac{1}{2}$ for isotopic substitution of one of the atomic species, e.g., ^{18}O for ^{16}O. Thus the measurement of a low value of α appreciably less than $\frac{1}{2}$ does not necessarily mean that strong-coupling effects are important. The assessment of strong-coupling

effects in a superconductor with many atomic species requires the knowledge of the reference oxygen isotope-effect exponent α_{rO}. In this work we have determined α_{rO} for $Ba_{1-x}K_xBiO_3$ from a joint inelastic-neutron-scattering (INS) and molecular-dynamics (MD) computer-simulation study. The result, $\alpha_{rO}=0.42 \pm 0.05$, is close to the most reliable value for α_{rO},[9] $\alpha_O=0.41\pm0.03$. We can conclude that $Ba_{1-x}K_xBiO_3$ is a weak-coupling superconductor. As discussed below, the large value of T_c in this material results from the large value of $\langle\omega\rangle$ associated with high-energy phonons involving oxygen vibrations and not from strong-coupling effects represented by $f(\lambda,\ldots,\mu^*)$.

$Ba_{0.6}K_{0.4}BiO_3$ samples were prepared by a melt-process technique. The ^{18}O isotopically exchanged sample could not be prepared by direct gas exchange because of the large sample size (nominally 100 g) with its large oxygen content relative to that of the exchange volume. The exchange was accomplished using a two-step process previously described.[9] The material, contained in gold foil, was heated to 700 °C in flowing nitrogen. It was held at this temperature for 8 h and then rapidly cooled to room temperature (RT). The system was then sealed and evacuated, followed by filling with $^{18}O_2$ gas (97.5% ^{18}O) from a liquid-$^{18}O_2$-containing bulb immersed in liquid nitrogen. The oxygen vacancies were filled by heating the sample to 400 °C, holding for 2 h, followed by cooling to RT with both cooling and heating done at 1 °C/min. The pressure remained at approximately 150 torr during this step. After seven cycles of this process the expected fraction of ^{18}O was calculated to be 82% (ignoring any gas exchange). Experimentally, using thermogravimetric analysis, the exchange fraction was found to be (74 ± 2)%.

INS experiments were performed using the HRMECS chopper spectrometer at the Intense Pulsed Neutron Source (IPNS) of Argonne National Laboratory. Pulsed spallation neutron sources have large fluxes of epithermal neutrons and are particularly well suited for investigation of high-energy ($20<E<80$ meV) oxygen phonons. The energy resolution (FWHM) varies from approximately 4% of the incident energy (110 meV) in the elastic region to $\sim$2.5% near the end of the neutron-energy-loss spectrum. Polycrystalline samples of $Ba_{0.6}K_{0.4}Bi^{16}O_3$ and $Ba_{0.6}K_{0.4}Bi^{18}O_3$, each about 100 g, were used in the measurements. To reduce multiple-phonon excitations, the samples were cooled to 15 K for the experiments.

For a multicomponent system, the neutron-weighted phonon DOS is given in the incoherent approximation by[19]

$$G(\omega)=e^{2\overline{W}}\sum_i \frac{c_i\sigma_i}{M_i}\langle(\hat{\mathbf{Q}}\cdot\hat{\mathbf{e}}_i)^2 e^{-2W_i}\rangle F_i(\omega)$$

$$\approx\sum_i \frac{c_i\sigma_i}{M_i}F_i(\omega)\,, \qquad (6)$$

where c_i, M_i, σ_i, and $F_i(\omega)$ are the concentration, mass, neutron-scattering cross section, and partial phonon DOS for the ith atomic species. In Eq. (6), $\hat{\mathbf{Q}}$, $\hat{\mathbf{e}}$, and $2\overline{W}$ are the unit scattering vector, polarization vector, and Debye-Waller exponent, respectively, and $\langle\cdots\rangle$ represents the average over all $\mathbf{Q}$ directions. The $(\hat{\mathbf{Q}}\cdot\hat{\mathbf{e}}_i)$ and Debye-Waller factors can be neglected in the present case because the measurements were made on polycrystalline materials over a wide range of Q at low temperatures.

MD simulations were performed with effective interatomic interactions consisting of Coulomb potentials due to charge-transfer effects, steric repulsion, and a charge-dipole interaction due to the large electronic polarizability of oxygen ions. The calculations were done with 540 particles for orthorhombic $BaBiO_3$ and with 625 particles for cubic $Ba_{0.6}K_{0.4}BiO_3$ using number densities and structural parameters determined from experiments.[3] In the case of $Ba_{0.6}K_{0.4}BiO_3$ the system was obtained by randomly replacing 40% of the Ba atoms with K atoms. Before calculating the phonon DOS, it was ensured that each system was dynamically stable in the appropriate symmetry. To establish the dynamical stability, an MD cell of fixed volume was constructed according to the crystal structure. The partial pair distribution functions and bond-angle distributions were calculated. The system was then slowly heated to 600 K and thermalized for several thousand time steps. After this it was run uninterruptedly for more than 30000 time steps and various structural correlations were calculated to examine the symmetry. The system was then cooled slowly and subjected to a steepest-descent quench, which is a mathematically well-defined method of examining the underlying mechanically stable structures. The pair-correlation functions and bond-angle distributions were calculated again to ascertain the symmetry of the MD system. After performing the above-mentioned procedure on both $BaBiO_3$ and $Ba_{0.6}K_{0.4}BiO_3$ it was determined that the resulting final symmetry was indeed the same as that of the starting structure. The phonon DOS were calculated by three different methods: (1) diagonalization of the dynamical matrix, (2) the equation-of-motion method, and (3) Fourier transformation of the velocity autocorrelation function. The results from these three methods are in agreement with one another.

Figure 1(a) shows the INS results for the neutron-weighted phonon DOS of ^{16}O and ^{18}O samples of $Ba_{1-x}K_xBiO_3$ for $x=0.4$. In the ^{16}O sample there are broad bands centered around 15, 30, and 60 meV. In addition, overlapping features in the DOS are observed around 26, 32–35, 42, and 55 meV. The overall shape of the phonon DOS for the ^{18}O sample is similar to that for the ^{16}O sample, except that the phonon spectrum above 20 meV is shifted to lower energies by 3–4 meV. This indicates that the spectrum above 20 meV arises mainly from the vibrations of oxygen atoms.

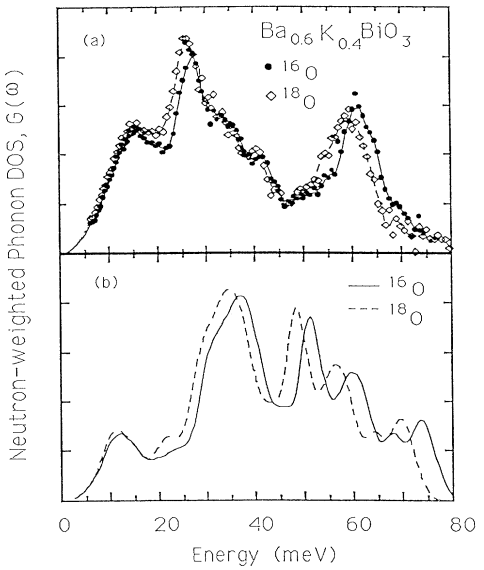

FIG. 1. Neutron-weighted phonon DOS $G(\omega)$ for ^{18}O and ^{16}O samples of $Ba_{0.6}K_{0.4}BiO_3$: (a) INS experimental values (the solid and dashed curves are guides to the eye), and (b) calculated from Eq. (6) using partial DOS $F_i(\omega)$ from the MD simulation, convolved with the experimental resolution function.

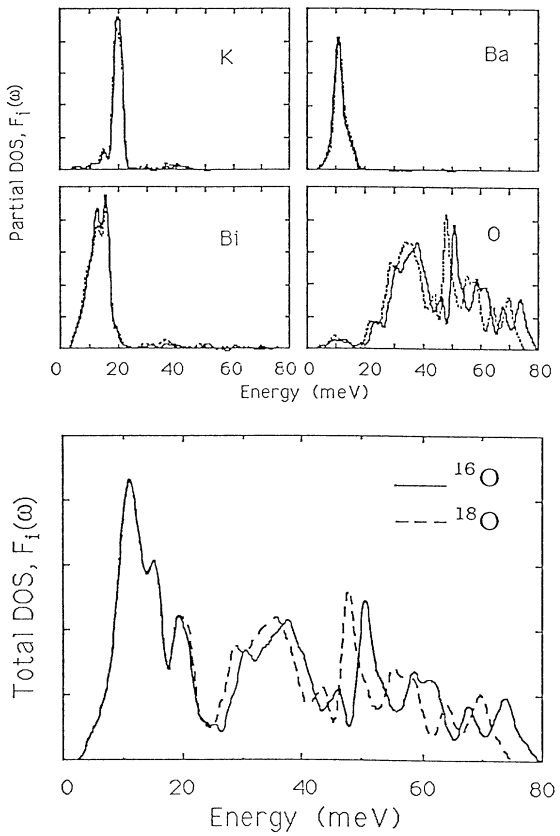

FIG. 2. MD partial and total phonon DOS for ^{18}O (dashed lines) and ^{16}O (solid lines) samples of $Ba_{0.6}K_{0.4}BiO_3$.

Results of the MD simulations for the partial DOS, $F_i(\omega)$, and the total phonon DOS, $F(\omega)=\sum_i F_i(\omega)$, of ^{16}O and ^{18}O samples are shown in Fig. 2. Clearly, the phonon spectra due to vibrations of oxygen atoms are confined to energies above 20 meV. In the MD spectra, there are phonon bands around 33 and 60 meV and, in addition, there are features around 43, 50, and 58 meV. The peaks around 33 and 60 meV are due to breathing modes of oxygen atoms around Bi and K (or Ba) atoms, respectively. The MD results for the partial DOS of Ba, K, and Bi show nearly overlapping peaks around 15 meV, which explains the origin of the observed phonon frequency band around 15 meV in the neutron data.

Using the partial DOS $F_i(\omega)$ from the MD simulation, we have calculated the neutron-weighted phonon DOS $G(\omega)$ from Eq. (6), shown in Fig. 1(b). As Fig. 1 shows, the overall agreement between the MD and INS results is quite good. The INS $G(\omega)$ displays three major phonon bands around 15, 30, and 60 meV. The corresponding features above 20 meV in the MD results have slightly higher energies. The INS value for the energy shift between the ^{16}O and ^{18}O phonon DOS, after accounting for the 74% ^{18}O in the isotopically substituted sample, agrees well with the value calculated from the MD results. The only discrepancy between the MD and INS results is that the former shows a peak around 50 meV whose amplitude in the experimental $G(\omega)$ is considerably smaller.

From the INS results for $G(\omega)$, we calculate a neutron-weighted first frequency moment

$$\langle\tilde{\omega}\rangle=\int d\omega\,\omega G(\omega)\Big/\int d\omega\,G(\omega).$$

The mass variation of $\langle\tilde{\omega}\rangle$ gives a neutron-weighted reference isotope-effect exponent 0.49 ± 0.05 after correcting for the 74% isotopic substitution in the ^{18}O sample. The MD results for $G(\omega)$ give a neutron-weighted exponent of 0.48. The excellent agreement between the INS and MD results for the neutron-weighted reference isotope-effect exponent confirms the reliability of the MD DOS.

We may now use the MD DOS to calculate from Eq. (3) the reference isotope-effect exponent, and obtain $\alpha_{rO}=0.42$. This value can be compared with the isotope-effect exponent derived from T_c measurements in our laboratory,[9] $\alpha_O=0.41\pm0.03$. We consider this value of α_O more reliable than other values in the literature[5,20] because it is the only measurement in which reproducibility was demonstrated by reexchanging with ^{16}O, and in which the composition was chosen to minimize systematic errors (that would lower the measured value of α_O) resulting from the loss of small amounts of potassium during processing. From Eq. (4) we derive

$\partial f/\partial \ln M_O = -0.1 \pm 0.06$, indicating that strong-coupling effects are not important in this material.[21]

In conclusion, this paper describes the first INS measurement on isotopically substituted samples of a high-T_c superconductor. The results indicate that oxygen phonons have energies in the range of 20–80 meV with significant peaks around 33 and 60 meV, in agreement with the results of MD simulation and tunneling measurements. By combining the INS and MD results, the reference isotope-effect exponent for oxygen is estimated to be 0.42, only slightly higher than the value for the isotope-effect exponent obtained experimentally in our laboratory (0.41). Because α_O is close to α_{rO}, we conclude that strong-coupling effects are small in this material. Had we compared the experimental value of α_O (0.41) with $\frac{1}{2}$ as is conventionally done, we would have arrived at the erroneous conclusion that $Ba_{1-x}K_xBiO_3$ is a strong-coupling superconductor. The correct analysis presented here demonstrates that $Ba_{1-x}K_xBiO_3$ is in fact a weak-coupling superconductor with large matrix elements coupling the electrons to high-energy phonons involving oxygen vibrations.

This work is supported by the U.S. DOE, BES-MS Contract No. W-31-109-ENG-38 and ER/DOE Cray at the National Magnetic Fusion Energy Computer Center, Livermore. W.J., B.D., D.R.R., and Y.Z. were supported by the NSF Superconductivity Center (DMR 88-09854), and M.H.D. by Fundação de Amparo à Pesquisa do Estado de São Paulo, Brazil.

---

[a]On leave from Instituto de Física e Química de São Carlos–Universidade de São Paulo, São Paulo, Brazil.

[1]L. R. Mattheiss *et al.*, Phys. Rev. B **37**, 3745 (1988).

[2]R. J. Cava *et al.*, Nature (London) **332**, 814 (1988).

[3]S. Pei *et al.*, Phys. Rev. B **41**, 4126 (1990).

[4]Y. J. Uemura *et al.*, Nature (London) **335**, 151 (1988).

[5]S. Kondoh *et al.*, Physica (Amsterdam) **157C**, 469 (1989).

[6]R. J. Birgeneau and G. Shirane, in *Physical Properties of High Temperature Superconductors,* edited by D. M. Ginsberg (World Scientific, Singapore, 1989), Vol. 1, Chap. 4, and references therein.

[7]H. Sato *et al.*, Nature (London) **338**, 241 (1989).

[8]C. P. Poole, Jr. *et al.*, *Copper Oxide Superconductors* (Wiley, New York, 1988), pp. 130 and 208, Table X.3, and references therein.

[9]D. G. Hinks *et al.*, Nature (London) **333**, 836 (1988).

[10]Z. Schlesinger *et al.*, Phys. Rev. B **40**, 6862 (1989).

[11]J. Zasadzinski *et al.*, Physica (Amsterdam) **158C**, 519 (1989).

[12]C.-K. Loong *et al.*, Phys. Rev. Lett. **62**, 2628 (1989).

[13]Q. Huang *et al.*, Nature (London) **347**, 369 (1990).

[14]See Eq. (22) of J. P. Carbotte, in Proceedings of the Symposium on the Manifestations of the Electron-Phonon Interaction in the CuO and Related Superconductors, edited by R. Baquero and J. P. Carbotte (World Scientific, Singapore, to be published); and J. P. Carbotte *et al.*, Phys. Rev. Lett. **66**, 1789 (1991). Depending on the approximations for the kernal in the Eliashberg equations, various analytic expressions for T_c (e.g., those given in Refs. 15–17) can be obtained. The isotope-effect exponents derived from these approximations can always be written in the form of Eq. (4).

[15]J. Bardeen *et al.*, Phys. Rev. **108**, 1175 (1957).

[16]W. L. McMillian, Phys. Rev. **167**, 331 (1968).

[17]P. B. Allen and R. C. Dynes, Phys. Rev. B **12**, 905 (1975).

[18]J. W. Garland, Jr., Phys. Rev. Lett. **11**, 114 (1963).

[19]D. L. Price and K. Sköld, in *Neutron Scattering,* edited by K. Sköld and D. L. Price (Academic, Orlando, FL, 1986), Pt. A, Chap. 1, p. 29.

[20]B. Batlogg *et al.*, Phys. Rev. Lett. **61**, 1670 (1988).

[21]P. B. Allen, Nature (London) **339**, 428 (1989).